Biodegradable Bicomponent Fibers from Renewable Sources: Melt-Spinning of Poly(lactic acid) and Poly[(3-hydroxybutyrate)-*co*-(3-hydroxyvalerate)]

Rudolf Hufenus,* Felix A. Reifler, Katharina Maniura-Weber, Adriaan Spierings, Manfred Zinn

PHBV is produced by bacteria as intracellular carbon storage. It is advantageous concerning biocompatibility and biodegradability, but its low crystallization rate hinders the melt-processing of fibers. This problem can be overcome by combining PHBV with PLA in a core/sheath configuration and introducing a new spin pack concept. The resulting PHBV/PLA bicomponent fibers show an ultimate tensile stress of up to 0.34 GPa and an E-modulus of up to 7.1 GPa. XRD reveals that PLA alone is responsible for tensile strength. In vitro biocompatibility studies with human fibroblasts reveal good cytocompatibility, making these fibers promising candidates for medical therapeutic approaches.

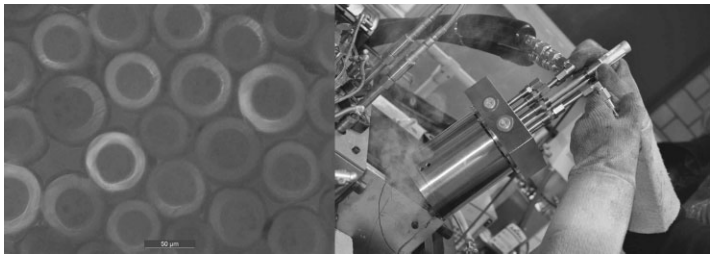

Introduction

Tailored biopolymer fibers play an important role in the medical field, e.g., as drug delivery systems, wound closure and healing products or surgical implant devices.[1] The major requirement for medical implants is that the polymers and their degradation products are biocompatible with the human body.[2,3] Desired properties comprise a minimal adverse effect on living tissue, i.e., the absence of inflammatory reaction or toxic response. In addition, bioresorbable fiber implants require a minimal tensile strength to fulfill their purpose in the body, and are expected to degrade after functional use[4,5] in order to avoid a second surgical intervention for removal.[6] Upon implantation into the body, biopolymers degrade into non-toxic by-products, either by hydrolysis or by enzymatic activity.[7] A biodegradable implant can be engineered to degrade at a rate that will slowly transfer load to a healing

R. Hufenus, F. A. Reifler
Laboratory for Advanced Fibers, Empa, Swiss Federal Laboratories for Materials Science and Technology, Lerchenfeldstrasse 5, CH-9014 St. Gallen, Switzerland
E-mail: rudolf.hufenus@empa.ch
K. Maniura-Weber
Laboratory for Materials/Biology Interactions, Empa, Swiss Federal Laboratories for Materials Science and Technology, Lerchenfeldstrasse 5, CH-9014 St. Gallen, Switzerland
A. Spierings
Inspire AG für Mechatronische Produktionssysteme, Institute for Rapid Product Development IRPD, Lerchenfeldstrasse 5, CH-9014 St. Gallen, Switzerland
M. Zinn
Laboratory for Biomaterials, Empa, Swiss Federal Laboratories for Materials Science and Technology, Lerchenfeldstrasse 5, CH-9014 St. Gallen, Switzerland

DOI: 10.1002/mame.201100063

tissue and/or as the basis for drug delivery systems.[4] The rate of biodegradation depends on the chemical nature of the polymer, on the polymer characteristics such as crystallinity, size, form, and number of crystallites, on the accessibility of the amorphous phase, and on the hydrophilicity.[5]

Polylactide (PLA) is the most widely used biodegradable polymer from renewable sources and is approved by the US Food and Drug Administration (FDA) for a number of clinical applications in humans.[2] It is regarded as a renewable plastic since its raw material (lactic acid) is produced by bacterial fermentation[8] from corn starch or sugar cane.[9,10] PLA has advantages such as thermoplastic processability and good mechanical properties.[11,12] The melt-spinning of PLA from different sources has been extensively studied.[13–15] PLA fibers are commercially available and have acceptable textile properties.[16] However, low melt strength, a narrow processing window, slow crystallization, and inherent brittleness are disadvantages that restrict large-scale applications of PLA.[12,17–19] The range of its applications as a functional biomaterial is limited by the acidity of its degradation by-product (lactic acid),[20] which might lower the local pH and thus trigger chronic inflammation of the surrounding tissue; therefore biocompatible buffering constituents have been added to the polymer.[21]

Polyhydroxyalkanoates (PHAs) are polyesters that are accumulated in bacteria as intracellular carbon and energy storage compounds.[22] Their polymer properties can be tailored and range from thermoplastic to elastomeric.[23] In contrast to PLA, PHAs degrade without forming toxic by-products.[24,25] Among PHAs, poly(3-hydroxybutyrate) (PHB) is the most frequently studied and the easiest to produce.[11,26] Low-molecular-weight PHB is occurring naturally in human blood, and its degradation product (3-hydroxybutyric acid) is a common metabolite in higher living beings.[27] PHB has been proposed for several biomedical applications[4] and is of great interest because of its biotechnological generation, its thermoplastic processability, its excellent biocompatibility, and its unique combination of biodegradability and hydrophobicity.[28,29] Compared to the PHB homopolymer, poly[(3-hydroxybutyrate)-*co*-(3-hydroxyvalerate)] (PHBV) is more flexible and easier to process.[30] Copolymerization leads to a lower melting temperature and a decrease of the crystallinity.[5,31] Completed with a plasticizer/softener and additives, PHBV is the most common commercial PHA-based product.[24] The rate of degradation can be controlled by varying the copolymer composition.[4] PHB and PHBV sutures implanted intramuscularly for up to one year did not cause any adverse effects.[32] The homopolymer poly(3-hydroxyvalerate) (PHV) is no suitable candidate for spinning because of its very low glass transition temperature of −14 °C.[33]

Taking the availability into account, PLA and PHAs are worthwhile candidates for biodegradable fibers from renewable sources. Regarding biocompatibility, biodegradable fibers completely based on PHAs, e.g., PHB or PHBV fibers, would be preferable. However, quality variations (molecular weight, purity) of the commercially available PHBs and PHBVs cause problems during melt-spinning.[25] In addition, rapid thermal degradation at temperatures just above the melting temperature, low melt elasticity, low crystallization rate due to a low nucleation density, and brittleness of native PHB and PHBV render a rather narrow processability window.[31,34–36] Up to now, melt-spinning of PHB and PHBV could only be achieved at a small scale applying special additives,[25,37] uncommon procedures[28,38] and complex post-treatment.[39–42]

In bicomponent melt-spinning two molten polymers are merged before or after leaving the spinneret capillary, so that the fibers consist of two joined components.[43] Hence, bicomponent fiber spinning provides an opportunity to combine the advantages of PLA (satisfactory tensile properties of the fibers) and PHAs (biocompatibility) and to overcome the problems described above. Bicomponent PLA/PHA fibers have been proposed to make environmentally degradable, disposable non-wovens,[44] and recently, core/shell fibers made from PLA and PHB by coaxial electrospinning for drug release purposes were presented.[45] PLA/PHB fibers are expected to show optimal performance with respect to mechanical properties and colonization by mouse or human fibroblasts, giving them a major interest for temporary textile implants.

Experimental Section

Polymers

Enmat Y1000 (T_m 165–175 °C, density 1.24 g · cm^{-3}, $\overline{M}_w \approx 490$ kDa), a PHBV powder with 8 mol% 3-hydroxyvalerate (3HV) content, provided by Tianan (Ningbo, China). For spinning experiments a pelletized version (Enmat Y1000P) was used.

PLA 6200D (T_m 160–170 °C, density 1.25–1.28 g · cm^{-3}, $\overline{M}_w \approx 100$ kDa), a fiber-grade PLA exhibiting a ratio of L/D stereochemical centers of approximately 98:2,[46] purchased from Natureworks (Minnetonka, USA).

Melt-Spinning Equipment

The fiber melt-spinning was carried out on Empa's custom-made pilot melt-spinning plant built by Fourné Polymertechnik (Alfter-Impekoven, Germany);[47] a schematic drawing is shown in Figure 1. This plant, with features corresponding to an industrial spinning line, enables the prototype production of mono-, bi-, and tricomponent fibers with various fiber cross-sections and material combinations with a throughput of 0.1–5 kg · h^{-1}. It comprises two screw extruders and one piston extruder. The diameters of the extruder screws are 13 mm (Part number 1 in Figure 1) and 18 mm (2), respectively, with a length-to-diameter (L/D) ratio of 25. In order

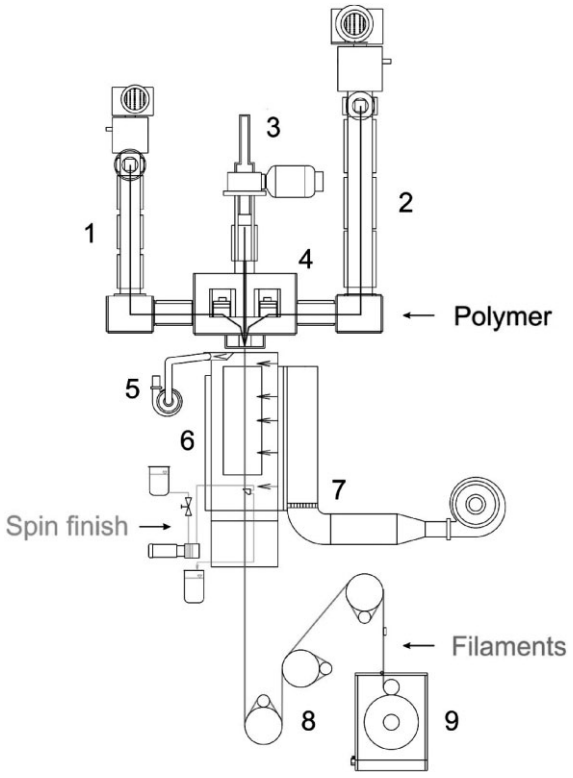

Figure 1. Schematic assembly of the pilot melt spinning plant (see text for an explanation of the numbered parts).

to produce tri-component fibers, an additional piston extruder (3) with a throughput of 1.5–15 $cm^3 \cdot min^{-1}$ is installed. Due to the possibility to fit sealing rings, also low-viscosity liquids can be processed. The maximum extrusion temperature is 400 °C. Spin pumps enable a constant mass flow of 0.5–40 $cm^3 \cdot min^{-1}$.

Depending on the type of fiber to be produced, various spin packs (4) can be installed. Evaporating monomers and oligomers are sucked in by an exhaust (5). The extrudate is spun into the 2.8 m free-fall section which is equipped with a removable or extendable chimney with a maximum temperature of 350 °C. The quenching chamber (6) has a maximum air flow of 520 $m^3 \cdot min^{-1}$ and a length of 1.4 m; its height within the free-fall section is variable in a continuous mode. The temperature of the quench air (7) can be adjusted between 8 and 160 °C, using either a two-step cooling system or a heater.

After cooling and, where applicable, wetting with a spin finish, the filaments are drawn by three heated godets (8). The maximum temperature of the godets is 210 °C, their speed can be varied between 100 and 1 800 rpm. The draw ratio, i.e., the ratio of speeds of draw and feed godets, can be chosen accordingly. Finally, a winder (9) with a maximum speed of 2 000 rpm is used to spool the filaments on a bobbin. Mono- and multifilaments with a fineness in the range of approx. 0.15–20 tex ($mg \cdot m^{-1}$) per filament can be produced.

For this study, the two polymers were melted using the single screw extruders (1, 2), and coaxially combined in a spinneret for bicomponent monofilaments with core/sheath-geometry. The die consisted of a tube with 0.4 mm inner diameter and 0.7 mm outer diameter within a 1.2 mm capillary. The draw ratios (ratio of speeds of draw and feed godets) were set between 1.5 and 6.

Polymer and Fiber Characterization

Samples were subjected to thermogravimetric analysis (TGA) using the TG 209 F1 Iris® instrument with Proteus Thermal Analysis software (Netzsch, Selb, Germany); heating rate: 10 °C · min^{-1} (25–800 °C); N_2 atmosphere (20 mL · min^{-1}). Differential scanning calorimetry (DSC) was performed employing a Mettler DSC 822e with Mettler STARe software package (Mettler-Toledo, Greifensee, Switzerland); heating rate: 20 °C · min^{-1} (25–350 °C); N_2 atmosphere (50 mL · min^{-1}). The crystallinity of the one-component fibers was estimated according to

$$w_c = \frac{(\Delta H_{melt} - \Delta H_{cc})}{\Delta H_{literature}} \times 100\% \quad (1)$$

in which w_c is the crystallinity, ΔH_{melt} the absolute value of the measured enthalpy of fusion, ΔH_{cc} the measured enthalpy of the cold crystallization and $\Delta H_{literature}$ the absolute value of the enthalpy of fusion of an ideal crystal. For the calculations, $\Delta H_{literature}$ of PLLA (93.7 J · g^{-1}[11]) and PHB (146 J · g^{-1}[48]), respectively, were used.

The molecular weight distribution of the polymers was determined by gel permeation chromatography (GPC) using the Viscotek GPCmax (Viscotek, Houston, USA). For the measurement, PLA was dissolved in chloroform (4–5 mg · mL^{-1}) at ambient temperatures, shaking it for 3 d. PHBV was dissolved in chloroform (4–5 mg · mL^{-1}) at 85 °C for 3 h, using pressure vials. At room temperature, the solutions were passed through a 0.45 μm syringe filter to remove non-dissolved material and dust, and injected with THF as eluent. Measurements were performed at 35 °C and analysis time was 50 min using a refractive-index (RI) detector. The samples were calibrated against 1–2 500 kDa polystyrene standards (PPS, Mainz, Germany).

The surface morphology of fibers was analyzed using the Hitachi FE-SEM S-4800 scanning electron microscope (Hitachi High-Technologies Europe, Krefeld, Germany). Sections of the fibers (thickness approx. 100 nm) were prepared with the microtome Leica EM UC6 (Leica Microsystems, Heerbrugg, Switzerland), attached onto copper mesh grids (Quantifoil Micro Tools, Jena, Germany) and analyzed using the scanning transmission electron microscope (STEM) option of the Hitachi S-4800.

For wide-angle X-ray diffraction (WAXD) analyses, fiber bundles of approx. 60 tex ($mg \cdot m^{-1}$), which consisted of 8–20 single filaments (depending on the fineness of the respective single filaments) were mounted on a custom-made sample holder. WAXD patterns were recorded on an Xcalibur PX four-circle single-crystal diffractometer (Oxford Diffraction Ltd, Yarnton, Oxfordshire, UK; κ-geometry; Mo $K_{\alpha 1}$ radiation, $\lambda = 0.70926$ Å, CCD area detection system) and evaluated by means of the CrysAlis Pro Data collection and processing software (Version 171.32.29, Oxford Diffraction Ltd., Yarnton, Oxfordshire, UK) and the XRD2DScan displaying and analyzing Software (Version 4.1, Alejandro Rodriguez Navarro; Universidad de Granada, Granada, Spain). Powder diffraction intensities were calculated from literature data using Cryscon (Version 1.2.1, Shape Software, Kingsport, TN, USA), a crystallography conversion utility.

The load/strain behavior of the fibers was evaluated using the Tensorapid 3 tensile tester (Uster Technologies, Uster, Switzerland); 500 N load cell; single-filament tests with 100 mm test length and a constant rate of extension of 100 mm · min^{-1}.

Degradation and Cytotoxicity Tests

To assess degradation, fiber samples of approx. 70–80 mg were weighed into centrifuge tubes (4 samples per fiber type). 10 mL of sterile NaCl solution (0.9%) was added to each tube. The influence of hydrolytic degradation on the physical properties was assessed by incubation in sterile solution at 37 °C for 4 weeks and subsequent mechanical analysis of the remaining fibers.

Cytotoxicity tests were carried out according to ISO 10993-5:2009.[49] Further, biocompatibility was assessed using normal human dermal fibroblasts (NHDF). Fiber samples were fixed in Cell Crown Inserts (Scaffdex, Tampere, Finland), sterilized with 70 vol% ethanol for 1 h and air dried under sterile conditions. Before cell seeding the samples were washed with phosphate-buffered saline (PBS) and Dulbecco's modified Eagle medium (DMEM, 10% fetal calf serum, 1% Penicillin-Streptomycin-Neomycin. Cell aggregates were prepared by centrifuging a suspension of 200 000 cells in a 15 mL tube (13 min, 60 g). The spherical cell pellets were incubated in the supernatant (37 °C, 5 h) and applied on top of the fiber samples in 4 mL of medium. Cells were fed every 3 d, fixed after 11 d and immuno-histochemically stained for cytoskeletal proteins vinculin, actin, and nucleus as described elsewhere.[50] Immunostained cells on the fibers were imaged using the fluorescence microscope Axio Imager M1 (Carl Zeiss, Germany).

Results and Discussion

Fiber Melt-Spinning

The viscometric average molecular weight of 490 kDa for the PHBV Enmat Y1000 powder gained from natural production was expected to be a good starting value for melt-spinning, but running an extruder with a polymer powder is rather difficult due to clogging of the powder at the extruder inlet. Thus most of the spinning trials were run with pellets. The drawbacks of the production of pellets are degradation (PHBV starts to degrade at 170 °C, while the processing temperatures lie at around 180 °C) and encased impurities (bio residues, degradation products). Inappropriate downstream processing can result in contamination of PHAs by bacterial compounds. As residual impurities in commercially available PHAs are from natural origin, they do not negatively influence biodegradability in the environment. However, they can negatively influence processability, either by catalyzing thermal degradation during extrusion,[51] or by clogging the extrusion filters and can also put biocompatibility at risk. Purification methods have been established to reduce the contamination of PHAs,[52] however, they are not applicable to pellets. Molecular weight and polydispersity are decisive factors regarding spinnability.[53] GPC measurements of the

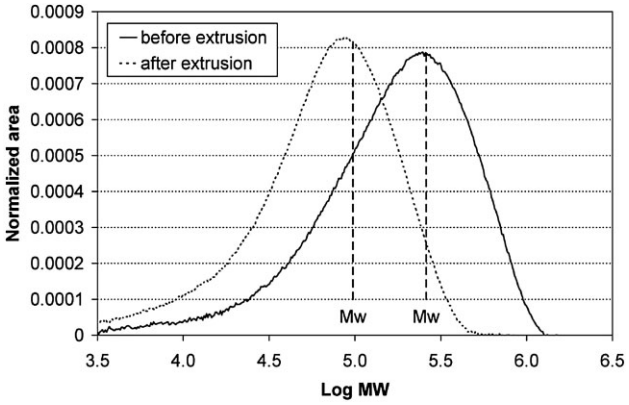

Figure 2. Molecular weight distribution of PHBV (Enmat Y1000P) before ($\overline{M}_w = 260$ kDa) and after ($\overline{M}_w = 97$ kDa) extrusion in the spinning line.

extruded pellets yielded a molecular weight of $\overline{M}_w = 260$ kDa, implying a reduction of 47% compared to the PHBV powder. After extrusion in the melt-spinning plant, it was reduced by another 63% down to $\overline{M}_w = 297$ kDa (Figure 2). By extrusion in the spinning line the polydispersity $\overline{M}_w/\overline{M}_n$ was reduced from 3.2 down to 2.7. Compared to PHAs, PLA is less susceptible to extrusion, as the degradation temperature (≈300 °C measured with TGA) lies far above the processing temperature of ≈190 °C. PLA 6200D by Natureworks could be spun to fibers with reasonable mechanical properties. Yet, due to thermal degradation during processing,[54] the molecular weight was reduced from $\overline{M}_w = 109$ kDa down to $\overline{M}_w = 90$ kDa (–17%) by extrusion in the melt-spinning plant. The polydispersity ($\overline{M}_w/\overline{M}_n$) changed from 2.1 to 2.0.

For reference purposes, pure PLA fibers have been produced (fibers 268, 293, 462, and 463 in Table 1).

As the biocompatibility of PHBV is better than that of PLA, having PHBV in the sheath of the bicomponent fiber would seem to be favorable. Nevertheless, the coextrusion of a PLA core and a PHBV sheath did not result in a processable fiber. Filaments of the bicomponent fiber could be wound up (fiber 460 in Table 1) with the help of a spin finish. However, the highest draw ratio achieved was only 1.5 because of the poor processability of PHBV. The low draw ratio and the thermal degradation of PHBV resulted in fibers with poor mechanical properties. For example, slightly pressing the fiber with a pin is sufficient to crack the fiber surface (Figure 3a and b). The analyses of the cross sections revealed impurities coming from the PHBV pellets used (Figure 3c and d). The stickiness of hot PHBV led to conglutination of the fibers on the godets. Even on the bobbin, the PHBV sheaths combined to one after ≈1 min. When trying to unwind the fibers, the sheath of an adjacent fiber was torn away from its core (Figure 3e and f). The only way to gain at least a few meters of the PLA/PHBV core/sheath fibers

Table 1. Extrusion parameters, draw ratio, and physical properties of the fibers produced. Stated are the composition of the core/sheath fibers (as assessed with TGA), the temperatures of the polymers leaving the extruder barrel, as well as the temperature of the spin pack. Fibers 459–465 were produced with a special spin pack comprising discrete temperature regimes using a cooling oil (oil temperature: 175 °C) that shields the PHBV from the spin pack temperature. The Young's Modulus was derived from superpositioned load-strain curves.

Fiber	Core		Sheath		Temperature [°C]			Draw ratio	Linear mass density [mg · m^{-1}]	Ultimate tensile stress [GPa]	Ultimate tensile strain [%]	Young's Modulus [GPa]
	Mater.	[wt%]	Mater.	[wt%]	Core	Sheath	Spin pack					
268	PLA	100	–	–	220	–	225	1.1	6.6	0.07 ± 0.02	–[a)]	3.6
293	PLA	100	–	–	220	–	225	4.5	1.25	0.39 ± 0.02	29 ± 2	5.9
378	PHBV	59	PLA	41	165	195	170	3	5.5	0.15 ± 0.01	30 ± 3	4.7
379	PHBV	62	PLA	38	165	195	170	3	6.0	0.17 ± 0.03	26 ± 9	5.3
380	PHBV	66	PLA	34	165	195	170	3	6.6	0.13 ± 0.02	31 ± 10	4.8
381	PHBV	69	PLA	31	165	195	170	3	7.2	0.14 ± 0.02	29 ± 7	4.5
394	PHBV	35	PLA	65	170	190	170	3	3.5	0.26 ± 0.03	38 ± 9	5.5
395	PHBV	36	PLA	64	170	190	170	3.5	3.0	0.32 ± 0.05	28 ± 5	7.1
396	PHBV	29	PLA	71	170	190	170	3.5	4.1	0.29 ± 0.02	34 ± 6	5.8
397	PHBV	22	PLA	78	170	190	170	3.5	4.6	0.29 ± 0.03	41 ± 6	6.4
459	PLA	49	PHBV	51	185	175	185	only mono-material free-fall fibers produced				
460	PLA	49	PHBV	51	185	175	185	1.5	6.8	0.08 ± 0.01	125 ± 29	2.9
462	PLA	100	–	–	185	–	190	6	5.1	0.41 ± 0.05	13 ± 3	6.6
463	PLA	100	–	–	185	–	190	6	6.1	0.41 ± 0.06	17 ± 4	6.0
464	PHBV	27	PLA	73	175	185	190	5.5	3.9	0.30 ± 0.02	23 ± 2	5.3
465	PHBV	29	PLA	71	175	185	190	5.5	4.7	0.34 ± 0.03	23 ± 2	6.0

[a)]not applicable as fiber was virtually not drawn (DR: 1.1), therefore lacking elastic properties.

consisted in unwinding them immediately after spinning, i.e., before the secondary crystallization took place.

As a next step, bicomponent fibers with a PHBV core and a PLA sheath were considered. Respective fibers with varying core/sheath ratios between 20:80 and 70:30 w/w were successfully spun (fibers 378–381, 394–397, and 464–465 in Table 1). Due to the poor processability of PHBV, the throughput of the metering pump eventually became lower than preset, leading to a reduced core to sheath ratio. As PHBV decomposes below 300 °C, and PLA starts to decompose above 300 °C, TGA is a valuable method to measure the core to sheath ratio of as-spun PHBV/PLA core/sheath fibers (Figure 4). Table 1 reveals the core/sheath ratios assessed with TGA. To validate these results, dimensions of the fiber cross sections (scanning electron micrographs) were measured.

Customized Spin Pack

As the ranges of the optimal processing temperatures of PLA and PHBV differ by about 20–30 °C, and in order to maintain and control the polymers as long as possible at their optimal temperatures during spinning, a highly integrated spin pack allowing the separate heating or cooling of up to three polymer channels was developed. In order to enhance the maximal temperature differences between these channels, it comprises a separate oil cooling and heating system for each channel to keep the polymer melt flows at different temperatures down to the spinneret plate. Each of the three channel sections is thermally isolated toward the other two sections by an internal narrow grid of convection channels[55–57] (Figure 5).

The spin pack was produced by selective laser melting (SLM),[58] an additive manufacturing process used for the fabrication of three-dimensional metal parts. By this it was possible to transfer the ideas already established for tooling for plastic injection molding applications – well known under the term "conformal cooling"[55,57–59] – to solve problems in fiber spinning. In the SLM process, a metal powder layer with a typical thickness in the range of 30–50 μm is generated on a metal base plate. Using a high energy laser beam, a cross section of a sliced 3D CAD data file is scanned, which leads to a full melting of the powder particles hit by the laser beam. Repeating this process layer by layer leads to a nearly fully dense 3D metal object.[60,61]

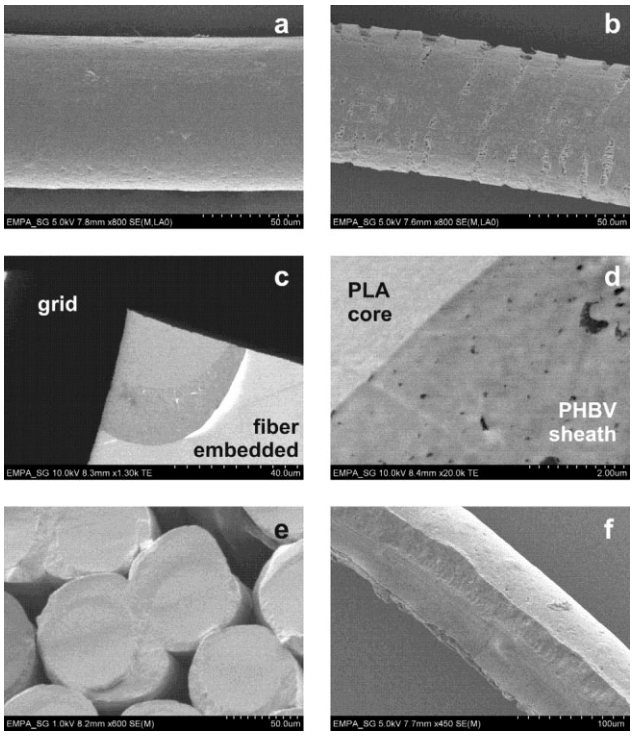

Figure 3. Scanning electron micrographs (fiber 460). (a, b) Surface of a PLA/PHBV core/sheath fiber before (a) and after (b) a feeble mechanical impact. (c, d) STEM pictures of the cross-section of a PLA/PHBV core/sheath fiber: Fiber cross-section attached onto a mesh grid (c), and intersection from the PLA core to the PHBV sheath (d); impurities in the PHBV sheath are evident (d). (e, f) Cross section (e) and top view (f) of conglutinated PLA/PHBV core/sheath fibers; separating the filaments resulted in excoriation (f).

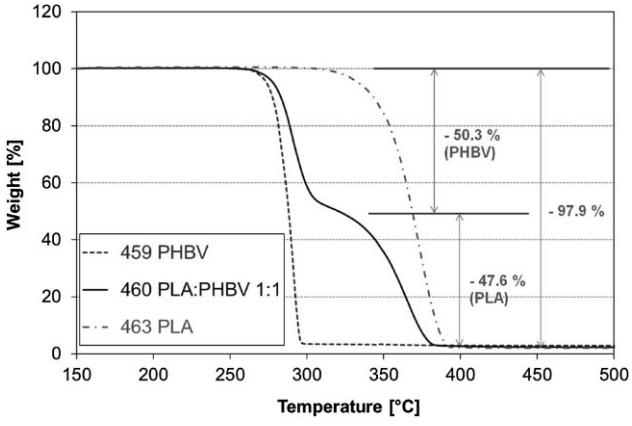

Figure 4. Thermogravimetric analysis (TGA) of extruded PHBV (trial no. 459), as well as spun PLA/PHBV core/sheath (trial no. 460) and PLA monocomponent fibers (trial no. 463). The core to sheath mass ratio can be calculated from the weight losses. The weight differences found experimentally (50.3 and 47.6% for PHBV and PLA, respectively) have to be scaled by a factor of (100/97.9), according to the total weight loss being 97.9% (remaining 2.1%: char residue). For fiber 460, this leads to a PLA/PHBV ratio of 49:51 wt%.

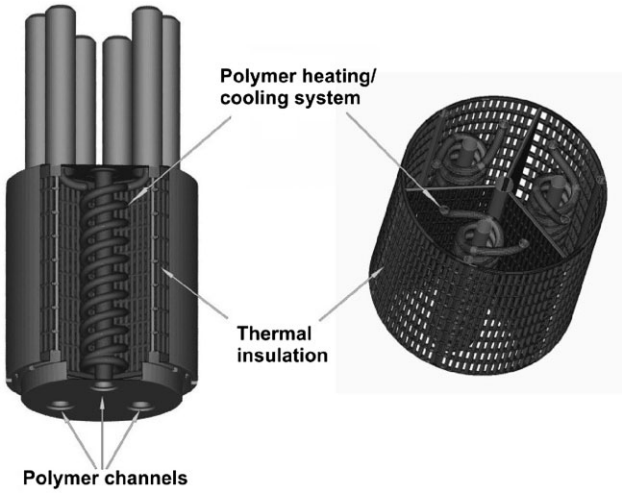

Figure 5. Left: Schematic of the highly integrated spin pack for three different polymers with heating/cooling channels and thermal insulation grid. The total volume of the spin pack is 350 cm^3. Right: Double helix system for cooling or heating and thermal insulation grid.

This additive process allows the fabrication of physical parts with a very high complexity[62] and even geometries that cannot be produced with conventional production techniques like drilling or milling. The following numbers will give an idea about the geometrical complexity of the spin pack design: the overall dimensions are 74 × 90 mm^2 (diameter × length), with a total length of the internal channels of about 13 m and a total cooling or heating surface of about 0.61 m^2 (Figure 5).

Before the new spin pack with different temperature regimes was introduced, the spin pack temperature could not excess 170 °C, for the PHBV not to decompose during spinning. As a result, spinning PLA at its optimal processing temperature (185 °C) was not possible, and the maximum achievable draw ratio was 3.5 (fibers 378–397 in Table 1). With the help of the new spin pack for some of the fibers used in this study (fibers 459–465 in Table 1), the temperature of the PHBV could be kept at its optimal processing temperature without reducing the processability of PLA, and a draw ratio of 5.5 became possible (fibers 464 and 465 in Table 1).

Tensile Properties

The tensile properties of melt spun fibers depend, amongst others, on the molecular orientation of the fibrous material which, in turn, is mostly determined by the draw ratio of the fiber.[63] Accordingly, it was found that the tensile strain (elongation at break) of the fibers depended mainly on the draw ratio (Figure 6a). With the exception of the poorly drawn PLA/PHBV core/sheath fiber (trial no. 460) with

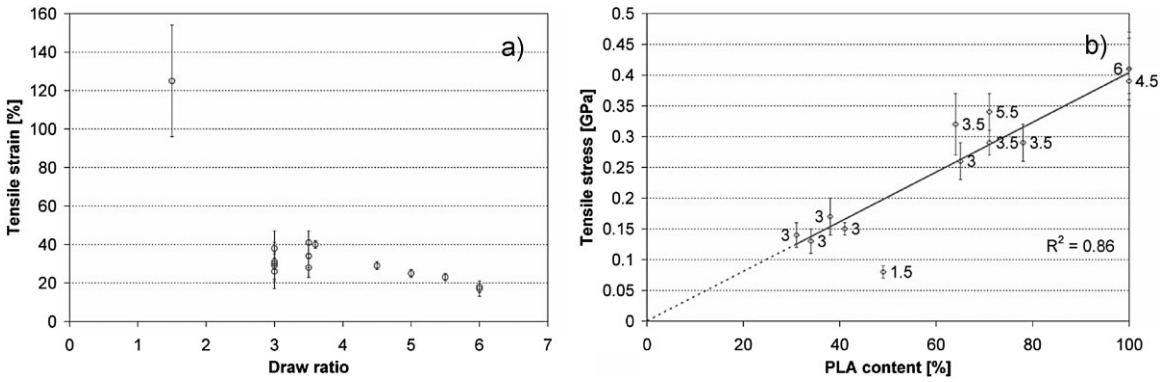

Figure 6. Tensile properties of the produced fibers. (a) Tensile strain (elongation at break) versus draw ratio of the PHBV/PLA bicomponent fibers. (b) Ultimate tensile stress versus PLA content of the PLA fibers and the PHBV/PLA bicomponent fibers. The numbers indicate the respective draw ratios.

comparatively low tensile strength, the ultimate tensile stress was roughly proportional to the PLA content of the PHBV/PLA core/sheath fibers (Figure 6b). Thus it can be concluded that the PLA component alone is responsible for the tensile strength, with no relevant contribution from the PHBV part. The Young's modulus (Table 1) was relatively low in case of the poorly drawn PLA/PHBV core/sheath fiber (trial no. 460), but increased with larger draw ratios. In contrast, the variation of the PLA content yielded diverse Young's moduli; a proportional dependency, however, was not detectable.

To prevent PHBV degradation, the temperature in the initial spin pack (without different temperature regimes) was fixed to 170 °C (Table 1), which is below the optimal processing temperature of PLA. As a consequence, the draw ratios obtainable for the bicomponent fibers 378–381 and 394–397 were as low as 3–3.5 (Table 1); applying higher draw ratios resulted in rupture of the fibers during spinning. Nevertheless, cyclic loading of these fibers showed a very promising elasticity. When a cyclic loading of up to 40% of the ultimate tensile stress was applied, a small hysteresis could be detected during the first cycle, followed by complete elastic recovery throughout the subsequent cycles (data not shown). After installation of the new spin pack, keeping the PLA and PHBV flows at different temperatures down to the spinneret (fibers 460–465) allowed to apply draw ratios of up to 6, resulting in improved tensile properties (Table 1). To test processability, sample fabrics were knitted from the bicomponent fibers 379 and 395. They proved to be strong enough for a successful construction of a textile fabric.

Crystallinity and Orientation

DSC measurements of the monocomponent fibers revealed a crystallinity of 42% for the PLA fiber (fiber no. 463, DSC peak temperature: 168.8 °C) and of 57% for the PHBV free-fall fiber (no. 459, DSC peak temperature: 173.7 °C). For the PLA/PHBV bicomponent fibers, however, DSC measurements cannot reveal the respective information for each of the two components, as their melting regions are too close to be distinguished. In contrast, WAXD using a 2D detector can provide valuable information about crystallinity and orientation of the crystals within the crystalline region of the fiber.[64] The PHBV used in this study, with a 3HV content of as low as 8 mol%, can be expected to crystallize in the PHB lattice.[65,66] X-ray diffraction data of PHB and PLA can be found in the literature[65]). Hence, the analysis of WAXD diffraction patterns will reveal the origin (PHBV or PLA) of the various features in the pattern.

In Figure 7, a selection of WAXD patterns is compiled. The PHBV free-fall fiber (459) and the bicomponent fibers show the diffraction pattern of orthorhombic α-PHB.[65,67] They reveal a very low crystal orientation of PHBV; the arcs are so expanded that they almost appear as closed rings. This explains why PHBV does not contribute to the tensile strength of the PHBV/PLA bicomponent fibers. Isothermal crystallization near the T_g followed by multiple one-step Drawing [41] or high draw ratios (up to 7)[25,28] were required to produce fibers with good crystal orientation from PHBV and native PHB, respectively. The maximum draw ratio of 5.5 achieved for the bicomponent experiments of this study was apparently not high enough for the PHBV to develop detectable orientation.

In the diffraction pattern of the PLA/PHBV bicomponent fiber with DR 1.5 (460) and of the bicomponent PHBV/PLA fiber with DR 3.0 (381) no reflections of the PLA component could be detected. Thus it can be concluded that the PLA stayed in its amorphous state due to the low draw ratios achieved. However, the pure PLA fiber (463) as well as the PHBV/PLA core/sheath fibers with DR 3.5 and 5.5 (396 and 465, respectively) showed crystalline patterns originating from fairly well oriented α-PLA;[68] the dots and small arcs in these diffraction patterns result from PLA only (Figure 7).

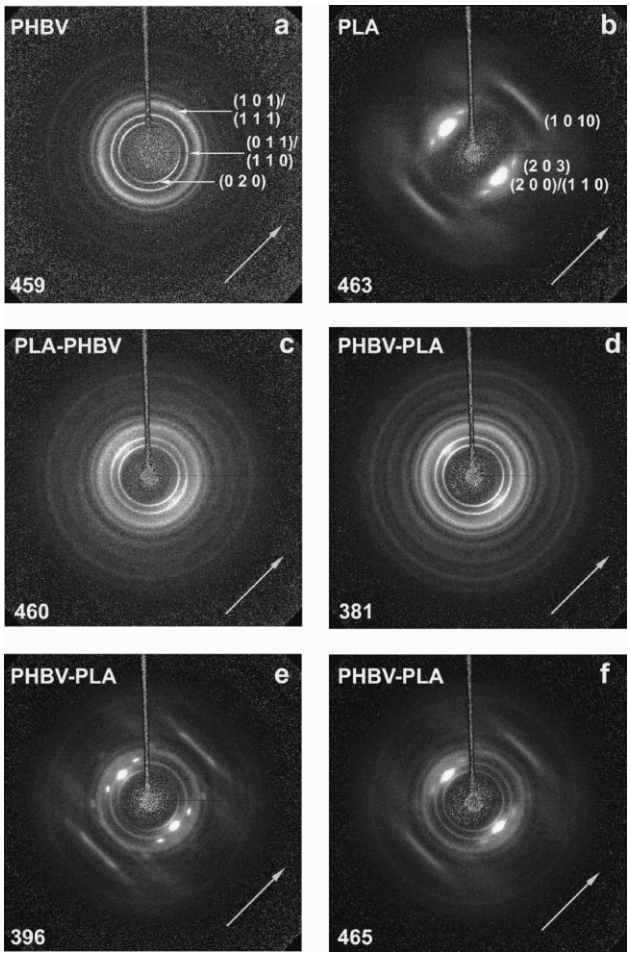

Figure 7. WAXD diffraction patterns of melt-spun biopolymer fibers. The arrows in the bottom right corner indicate the direction of the respective fiber axes. (a) PHBV free-fall fiber (459); free-fall fibers are collected after the spinneret, before they strike the first godet. Diffraction pattern: α-PHB;[65,67] indexing of the strongest reflections according to the literature.[67] (b) PLA, DR 6 (463). Diffraction pattern: α-PLA; indexing of the strongest reflections according to the literature.[68] (c) PLA/PHBV 49:51, DR 1.5 (460). (d) PHBV/PLA 69:31, DR 3.0 (381). (e) PHBV/PLA 29:71, DR 3.5 (396). (f) PHBV/PLA 29:71, DR 5.5 (465).

Degradation in an Abiotic System

Biopolymer fibers degrade either through an erosion process that starts on the exterior surface and continues until the fiber has been totally absorbed, or by a bulk erosion mechanism leading to autocatalytic hydrolysis that starts in the center of the fiber.[7] Abiotic (sterile) degradation tests on bicomponent fibers with PLA as the sheath material in non-buffered, isotonic salt solution showed a drop of the pH to as low as 4.7, which is expected to correlate with the release of lactic acid upon degradation of the material.

Because PLA undergoes bulk degradation, the molecular weight of the polymer commences to decrease immediately upon contact with water (3–8% loss of $\overline{M}_w$ detected after 4 weeks of incubation), leading to a decrease in tensile strength (ultimate tensile stress reduction of 5–33%, Figure 8a). A weight loss was not detected, which leads to the assumption that the mass did not change significantly until the molecular chains were reduced enough in length to freely diffuse out of the polymer matrix.[21]

Cytocompatibility

In vitro biocompatibility studies with human dermal fibroblasts showed no toxicity of the bicomponent fibers despite the presumed production of acidic lactic acid resulting from the assumed degradation of the fibers. Extract tests according to ISO 10993-5:2009[49] showed no adverse effect on 3T3 cells (Figure 8b). Fibroblasts growing out from cell re-aggregates adhered to the fibers and grew along single filaments, covering them well after a cultivation period of 1 week (Figure 8c and d). The well expressed cytoskeleton showed that cells adhere on the fibers, making them good candidates for medical therapeutic approaches. Neither pure PLA fibers nor PHBV/PLA core/sheath fibers turned out to be toxic.

Conclusion

Bicomponent melt-spinning to combine the properties of PLA and PHBV was applied. Conglutination due to secondary crystallization of native PHBV made it impossible to melt-draw bicomponent fibers with PLA core and PHBV sheath, but fibers with a PHBV core and a PLA sheath were successfully spun. To keep the temperature of PHBV substantially lower than the PLA temperature during melt-spinning, a special spin pack was developed. Hence, higher draw ratios became possible. The bicomponent fibers with PLA as a sheath material achieved ultimate tensile stresses of up to 0.34 GPa and a Young's modulus of up to 7.1 GPa, and proved to be strong enough for a successful construction of a textile fabric.

The ultimate tensile stress of the PHBV/PLA core/sheath fibers was roughly proportional to the PLA content, indicating that the PHBV did not contribute to the tensile strength. This can be explained by the fact that the PHBV component developed no molecular orientation, while the PLA component was fairly well oriented, as revealed by WAXD analysis.

In vitro biocompatibility studies with human dermal fibroblasts revealed no toxicity of the fibers. Cells proliferated well along the individual fibers and spanned fiber intersections after 10 d of cultivation. Abiotic degradation tests showed a decrease of molecular weight and reduction in tensile strength of up to 33% after 4 weeks of incubation. The good cytocompatibility that has been found makes

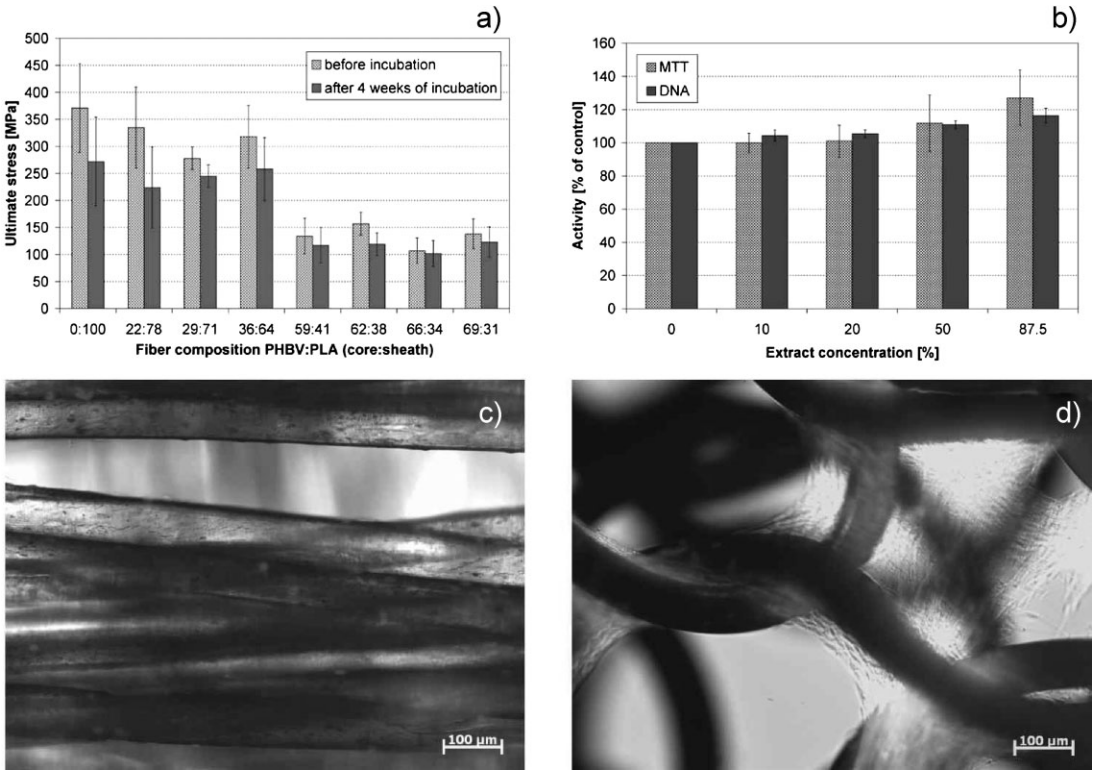

Figure 8. Fiber degradation and cytocompatibility: (a) Ultimate tensile stress of some bicomponent fibers before and after 4 weeks of incubation in an isotonic sodium chloride solution. (b) Cytotoxicity assay of pure PLA fiber (462) according to ISO 10993-5:2009;[49] MTT and DNA were measured in cell cultures that had the indicated fractions of polymer fiber extracts added ($n = 3$). (c) Overlay of light and fluorescence micrographs shows cells on PLA/PHBV core/sheath fibers (no. 460) which are stained for nuclei. (d) Cells on pure PLA fibers (no. 463) showing cell nuclei, actin (cytoskeleton), and vinculin staining (focal adhesions).

PHBV/PLA bicomponent fibers promising candidates for medical therapeutic approaches.

Acknowledgements: The authors thank Benno Wüst for operating the spinning plant, Bernhard Weisse and Pierluigi Barbadoro for mechanical characterization, Patrick Rupper and Käthe Meyer for SEM support, Sabyasachi Gaan for TGA measurements, Sandro Dilettoso for degradation tests, Matthijs de Geus for GPC measurements, Stefanie Lischer for biocompatibility assessment, Yajing Wang for DSC analysis and performing WAXD experiments, Stefan Buob for his support in spin pack design and production, Thomas Weber, Christian Baerlocher and Walter Steurer of the Laboratory of Crystallography (Department of Materials, ETH Zürich, Switzerland) for providing access to their WAXD equipment and for generous support.

Received: February 10, 2011; Revised: May 11, 2011; Published online: July 25, 2011; DOI: 10.1002/mame.201100063

Keywords: bicomponent fibers; biocompatibility; biopolyester; biopolymers; processing

[1] K. Van de Velde, P. Kiekens, *Polym. Test.* **2002**, *21*, 433.
[2] W. He, Y. Feng, Z. Ma, S. Ramakrishna, "Polymers for Tissue Engineering," in: *Polymers for Biomedical Applications* (Eds. A. Mahapatro, A. S. Kulshrestha), American Chemical Society, Washington, DC **2008**, p. 310 ff.
[3] S. Ramakrishna, J. Mayer, E. Wintermantel, K. W. Leong, *Compos. Sci. Technol.* **2001**, *61*, 1189.
[4] J. C. Middleton, A. J. Tipton, *Biomaterials* **2000**, *21*, 2335.
[5] J. P. Penning, H. Dijkstra, A. J. Pennings, *Polymer* **1993**, *34*, 942.
[6] K. A. Athanasiou, C. M. Agrawal, F. A. Barber, S. S. Burkhart, *Arthroscopy* **1998**, *14*, 726.
[7] S. Weinberg, M. W. King, "Medical Fibers and Biotextiles," in: *Biomaterials Science – An Introduction to Materials in Medicine*, 2nd edition (Eds. B. D. Ratner, A. S. Hoffman, F. J. Schoen, J. E. Lemons), Elsevier Academic Press, San Diego **2004**, p. 86 ff.
[8] R. Auras, B. Harte, S. Selke, *Macromol. Biosci.* **2004**, *4*, 835.
[9] R. E. Drumright, P. R. Gruber, D. E. Henton, *Adv. Mater.* **2000**, *12*, 1841.
[10] Y. Tokiwa, A. Jarerat, *Biotechnol. Lett.* **2004**, *26*, 771.
[11] B. M. P. Ferreira, C. A. C. Zavaglia, E. A. R. Duek, *J. Appl. Polym. Sci.* **2002**, *86*, 2898.
[12] L. T. Lim, R. Auras, M. Rubino, *Prog. Polym. Sci.* **2008**, *33*, 820.
[13] J. A. Cicero, J. R. Dorgan, *J. Polym. Environ.* **2001**, *9*, 1.
[14] L. Fambri, A. Pegoretti, R. Fenner, S. D. Incardona, C. Migliaresi, *Polymer* **1997**, *38*, 79.
[15] G. Schmack, D. Jehnichen, R. Vogel, B. Tändler, R. Beyreuther, S. Jacobsen, H. G. Fritz, *J. Biotechnol.* **2001**, *86*, 151.
[16] V. K. Kothari, S. Yadav, *Asian Text. J.* **2008**, *17*, 29.
[17] A. K. Bledzki, A. Jaszkiewicz, *Compos. Sci. Technol.* **2010**, *70*, 1687.

[18] A. H. Pei, Q. Zhou, L. A. Berglund, *Compos. Sci. Technol.* **2010**, *70*, 815.
[19] R. Wang, S. Wang, Y. Zhang, *J. Appl. Polym. Sci.* **2009**, *113*, 3095.
[20] G. S. Kwon, D. F. Ferguson, "Biodegradable Polymers for Drug Delivery Systems," in: *Biomedical Polymers*, 1st edition *(Ed.*, M. Jenkins), Woodhead Publishing, Cambridge **2007**, p. 83 ff.
[21] C. M. Agrawal, K. A. Athanasiou, *J. Biomed. Mater. Res.* **1997**, *38*, 105.
[22] K. Sudesh, H. Abe, Y. Doi, *Prog. Polym. Sci.* **2000**, *25*, 1503.
[23] M. Zinn, B. Witholt, T. Egli, *Adv. Drug Del. Rev.* **2001**, *53*, 5.
[24] *Biodegradable Plastics – Developments and Environmental Impacts;*, Environment Australia, Melbourne **2002**, p 66.
[25] R. Vogel, B. Tändler, D. Voigt, D. Jehnichen, L. Häussler, L. Peitzsch, H. Brünig, *Macromol. Biosci.* **2007**, *7*, 820.
[26] G. Q. Chen, *Chem. Soc. Rev.* **2009**, *38*, 2434.
[27] T. Freier, C. Kunze, C. Nischan, S. Kramer, K. Sternberg, M. Sass, U. T. Hopt, K. P. Schmitz, *Biomaterials* **2002**, *23*, 2649.
[28] C. Schmack, D. Jehnichen, R. Vogel, B. Tändler, *J. Polym. Sci. Part B: Polym. Phys.* **2000**, *38*, 2841.
[29] M. Zinn, R. Hany, *Adv. Eng. Mater.* **2005**, *7*, 408.
[30] E. Chiellini, R. Solaro, *Adv. Mater.* **1996**, *8*, 305.
[31] K. Arakawa, T. Yokohara, M. Yamaguchi, *J. Appl. Polym. Sci.* **2008**, *107*, 1320.
[32] E. I. Shishatskaya, T. G. Volova, A. P. Puzyr, O. A. Mogilnaya, S. N. Efremov, *J. Mater. Sci. Mater. M.* **2004**, *15*, 719.
[33] A. Steinbüchel, G. Schmack, *J. Environ. Polym. Degrad.* **1995**, *3*, 243.
[34] P. J. Barham, A. Keller, *J. Polym. Sci. Part B: Polym. Phys.* **1986**, *24*, 69.
[35] I. Chodak, R. S. Blackburn, "Poly(hydroxyalkanoates) and Polycaprolactone," in: *Biodegradable and Sustainable Fibres*, 1st edition *(Ed.*, R. S. Blackburn), Woodhead Publishing Limited, Cambridge **2005**, p. 221 ff.
[36] R. Vogel, B. Tändler, L. Häussler, D. Jehnichen, H. Brünig, *Macromol. Biosci.* **2006**, *6*, 730.
[37] C. Hinüber, L. Häussler, R. Vogel, H. Brünig, C. Werner, *Macromol. Mater. Eng.* **2010**, *295*, 585.
[38] R. Vogel, D. Voigt, B. Tändler, U. Gohs, L. Häussler, H. Brünig, *Macromol. Biosci.* **2008**, *8*, 426.
[39] T. Iwata, *Macromol. Biosci.* **2005**, *5*, 689.
[40] T. Iwata, Y. Aoyagi, M. Fujita, H. Yamane, Y. Doi, Y. Suzuki, A. Takeuchi, K. Uesugi, *Macromol. Rapid Commun.* **2004**, *25*, 1100.
[41] T. Tanaka, M. Fujita, A. Takeuchi, Y. Suzuki, K. Uesugi, K. Ito, T. Fujisawa, Y. Doi, T. Iwata, *Macromolecules* **2006**, *39*, 2940.
[42] T. Tanaka, T. Yabe, S. Teramachi, T. Iwata, *Polym. Degrad. Stabil.* **2007**, *92*, 1016.
[43] S. Houis, F. Schreiber, T. Gries, "*Fibre-Table according to P.-A. Koch: Bicomponent Fibres*,", Shaker, Aachen **2008**.
[44] I. Noda, E. B. Bond, D. H. Melik, (Procter & Gamble), *US* 6905987 (2005).
[45] C. Wang, K. W. Yan, Y. D. Lin, P. C. H. Hsieh, *Macromolecules* **2010**, *43*, 6389.
[46] J. A. Cicero, J. R. Dorgan, J. Janzen, J. Garrett, J. Runt, J. S. Lin, *J. Appl. Polym. Sci.* **2002**, *86*, 2828.
[47] S. Houis, M. Schmid, J. Lübben, *J. Appl. Polym. Sci.* **2007**, *106*, 1757.
[48] L. M. W. K. Gunaratne, R. A. Shanks, *Eur. Polym. J.* **2005**, *41*, 2980.
[49] *ISO 10993-5:2009. Biological evaluation of medical devices – Part 5: Tests for* in vitro *cytotoxicity*. ISO International Organization for Standardization, Geneva, **2009**.
[50] A. K. Born, M. Rottmar, S. Lischer, M. Pleskova, A. Bruinink, K. Maniura-Weber, *Eur. Cells Mater.* **2009**, *18*, 49.
[51] L. Chen, P. Wang, Y. Chen, Y. Zhang, M. Zhu, *Front. Chem. Chin.* **2008**, *3*, 445.
[52] P. Furrer, M. Zinn, S. Panke, "Polyhydroxyalkanoate and its Potential for Biomedical Applications," in: *Natural-Based Polymers for Biomedical Applications*, 1st edition *(Ed.*, R. L. Reis), Woodhead Publishing, Cambridge **2008**, p. 416 ff.
[53] G. Schmack, B. Tändler, G. Optiz, R. Vogel, H. Komber, L. Häussler, D. Voigt, S. Weinmann, M. Heinemann, H. G. Fritz, *J. Appl. Polym. Sci.* **2004**, *91*, 800.
[54] A. K. Sugih, F. Picchioni, H. J. Heeres, *Eur. Polym. J.* **2009**, *45*, 155.
[55] D. E. Dimla, M. Camilotto, F. Miani, *J. Mater. Process. Technol.* **2005**, *164*, 1294.
[56] T. Dormal, presented at the *2nd International Conference on Additive Technologies*, Ptuj, Slovenia, **2008**.
[57] A. V. Villalon, *Master Thesis*, North Carolina State University, Raleigh **2005**.
[58] G. N. Levy, R. Schindel, J. P. Kruth, *"CIRP Ann. Manuf. Technol.* **2003**, *52*, 589.
[59] F. Herzog, *Casting Plant Technol.* **2008**, *1*, 18.
[60] A. B. Spierings, N. Herres, G. Levy, *Rapid Prototyping J.* **2011**, *17*, 195.
[61] A. B. Spierings, G. Levy, in *Proceedings of the Annual International Solid Freeform Fabrication Symposium*, Vol. 20 (Ed. D. L. Bourell), Austin, Texas: **2009**, pp. 342.
[62] T. Vilaro, S. Abed, W. Knapp, in *Assises Européennes de Prototypage Rapide*, Vol. *12*, **2008**.
[63] F. Fourné, "*ynthetic Fibers*,", 1st edition, Hanser Publishers, Munich **1999**.
[64] J. W. S. Hearle, "Fibers, Structure," in: *Ullmann's Fibers*, Vol. 1, Wiley-VCH, Weinheim **2008**, p. 39 ff.
[65] P. Pan, Y. Inoue, *Prog. Polym. Sci.* **2009**, *34*, 605.
[66] N. Yoshie, M. Saito, Y. Inoue, *Macromolecules* **2001**, *34*, 8953.
[67] J. Cornibert, R. H. Marchessault, *J. Mol. Biol.* **1972**, *71*, 735.
[68] T. Miyata, T. Masuko, *Polymer* **1997**, *38*, 4003.